Robust Distributed Guidance and Control of Multiple Autonomous Surface Vehicles based on Extended State Observers and Finite-set Model Predictive Control

Haoliang Wang
School of Marine Electrical Engineering
Dalian Maritime University
Dalian 116026, P. R. China
Email: haoliang.wang12@dlmu.edu.cn

Jizhou Jiang
School of Marine Electrical Engineering
Dalian Maritime University
Dalian 116026, P. R. China
Email: jizhoujiang@126.com

Wentao Wu
School of Marine Electrical Engineering
Dalian Maritime University
Dalian 116026, P. R. China
Email: wuwentaodlmu@gmail.com

Lu Liu
School of Marine Electrical Engineering
Dalian Maritime University
Dalian 116026, P. R. China
Email: wendaoerji@163.com

Dan Wang
School of Marine Electrical Engineering
Dalian Maritime University
Dalian 116026, P. R. China
Email: dwangdl@gmail.com

Zhouhua Peng
School of Marine Electrical Engineering
Dalian Maritime University
Dalian 116026, P. R. China
Email:zhpeng@dlmu.edu.cn

***Abstract*—This paper is concerned with the guidance and control design for a swarm of multiple under-actuated autonomous surface vehicles subject to unmeasured velocities of neighbors, system uncertainties and ocean disturbances. A robust distributed guidance and predictive control architecture is presented to achieve a desired formation along a parameterized path. Specifically, a robust distributed constant bearing guidance law is designed based on extended state observers. Then, optimized surge speed and heading controllers are designed based on finite-set model predictive control for selecting optimal actions within finite control sets and extended state observers for recovering the unmeasured yaw rate and unknown model. Simulation results demonstrate the effectiveness of the proposed robust distributed cooperative guidance and control methods for path-guided formation maneuvering of multiple under-actuated autonomous surface vehicles.**

***Index Terms*—Autonomous surface vehicles, distributed cooperative guidance, extended state observer, finite-set model predictive control**

I. Introduction

In recent years, formation control of multiple autonomous surface vehicles (ASVs) has drawn compelling interests and a large number of formation control methods are available [1]–[14], ranging from leader-follower approach [15], [16], behavior approach, potential functions [3], and graph-based mechanism [1]–[9]. In particular, graph-based distributed formation control methods has been well studied. Distributed formation control of fully-actuated ASVs based on local information of neighboring vehicles has been presented in [1]–[3], [7]. In [8], a path-guided time-varying formation controller with the capability of collision avoidance and connectivity maintenance is proposed for each ASV. In [9], a path-guided distributed containment controller is proposed for each ASV guided by multiple virtual leaders. The limitations are stated as follows. Firstly, the velocities of neighbours and formation derivations are required at the kinematic level. Secondly, the kinetic control law may not lead to optimal performance in the presence of input constraints.

Motivated by the above observations, this paper aims to address the cooperative guidance and control of multiple under-actuated ASVs subject to unmeasured velocities of neighbors, internal model uncertainties and external disturbances. The group is guided by a parameterized path which is known in advance. A robust distributed guidance and predictive control architecture is presented to achieve a desired formation along the parameterized path. More specifically, a robust distributed constant bearing guidance law is designed based on an extended state observer (ESO). At the control loop, robust predictive surge speed and heading controllers are designed under the assumption that the total disturbance is invariant in the prediction horizon. The optimal actions within finite control sets are selected based on finite-set model predictive control (FS-MPC). The effectiveness of the proposed robust

This work was supported in part by the National Natural Science Foundation of China under Grants 61673081, 51979020, 51909021, 51939001, and in part by Science and Technology Fund for Distinguished Young Scholars of Dalian under Grant 2018RJ08, and in part by the Stable Supporting Fund of Science and Technology on Underwater Vehicle Technology JCKYS2019604SXJQR-01, and in part by the Supporting Program for High-level Talent in Transportation Department under Grant 2018-030, and in part by the National Key Research and Development Program of China under Grant 2016YFC0301500, and in part by the Fundamental Research Funds for the Central Universities under Grant 3132019319, 3132020101, and in part by China Postdoctoral Science Foundation 2019M650086.

978-1-7281-9888-0/20/$31.00 ©2020 IEEE

distributed guidance and predictive control scheme is verified via simulations.

II. Preliminaries and Problem Description

A. Basic concepts and results in graph theory

A weighted directed graph is denoted by $\mathcal{G} = \{\mathcal{V}, \mathcal{E}, \mathcal{A}\}$ with a node set $\mathcal{V} = \{n_1, n_2, ..., n_N\}$. The set $\mathcal{E} = \{(n_i, n_j) \in \mathcal{V} \times \mathcal{V}\}$ is an edge set, (n_i, n_j) denotes that i-th ASV sends information to j-th ASV ($i \neq j$). A adjacency matrix $\mathcal{A} = [a_{ij}] \in \Re^{N \times N}$ with nonnegative elements a_{ij} shows communication links between vehicles. If $(n_j, n_i) \in \mathcal{E}$, $a_{ij} = 1$; otherwise, $a_{ij} = 0$. The Laplacian matrix of $\mathcal{G}$ is defined as $\mathcal{L} = \mathcal{D} - \mathcal{A}$ where $\mathcal{D}$ is called a degree matrix of $\mathcal{G}$ with $\mathcal{D} = \text{diag}\{d_1, d_2, ..., d_N\} \in \Re^{N \times N}$ with $d_i = \sum_{j=1}^{N} a_{ij}$, $i = 1, ..., N$.

Assumption 1. The graph $\mathcal{G}$ contains a spanning tree with the root node being the node n_0.

B. Problem description

Consider a system consisting of N ASVs with a three degrees of freedom model as

$$\begin{cases} \dot{x}_i = u_i \cos(\psi_i) - v_i \sin(\psi_i), \\ \dot{y}_i = u_i \sin(\psi_i) + v_i \cos(\psi_i), \\ \dot{\psi}_i = r_i, \end{cases} \tag{1}$$

and

$$\begin{cases} m_{iu}\dot{u}_i = f_{iu}(u_i, v_i, r_i) + \tau_{iu} + \tau_{iwu}(t), \\ m_{iv}\dot{v}_i = f_{iv}(u_i, v_i, r_i) + \tau_{iwv}(t), \\ m_{ir}\dot{r}_i = f_{ir}(u_i, v_i, r_i) + \tau_{ir} + \tau_{iwr}(t), \end{cases} \tag{2}$$

where (x_i, y_i) denotes the position of i-th ASV along X_E and Y_E axis, ψ_i denotes the heading angle in the earth-fixed reference frame $\{E\}$; u_i,v_i and r_i denote the surge speed, sway speed and angular rate in the body-fixed reference frame $\{B\}$, respectively; m_{iu},m_{iv} and m_{ir} denote the inertia terms; $f_{iu}(\cdot)$, $f_{iv}(\cdot)$ and $f_{ir}(\cdot)$ are nonlinear functions of model uncertainties; τ_{iu} and τ_{ir} are control input of ASVs; τ_{iwu}, τ_{iwv} and τ_{iwr} are the ocean disturbances.

Consider a virtual leader moving along a parameterized path $p_0(\theta) = [x_0(\theta), y_0(\theta)]^T \in \Re^2$, where $\theta \in \Re$ is a path variable; $p_0(\theta)$ is the position of virture leader.

A geometrical illustration of the path-guided formation control is shown in Fig.1. The control objective is to achieve a distributed formation control of multiple ASVs guided by the parameterized path with constrained control inputs.

III. Distributed Cooperative Guidance Law Design

This section presents the guidance law design for tracking a parameterized path with the fixed formation.

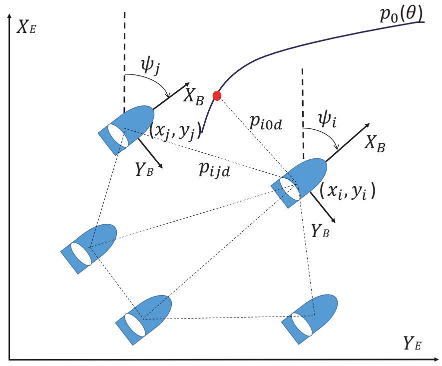

Fig. 1. Path-guided distributed formation control of ASVs

A. Guidance law design

At first, a formation position error of i-th ASV based on the information of neighbors is defined as

$$\begin{aligned} z_i = &\textstyle\sum_{j=1}^{N} a_{ij}(p_i - p_j - p_{ijd}) \\ &+ a_{i0}(p_i - p_0(\theta) - p_{i0d}), \end{aligned} \tag{3}$$

where p_i, p_j are the position of i-th ASV and j-th ASV; $p_{ijd} = p_{id} - p_{jd}$ is a relative deviation with p_{id}, $p_{jd} \in \Re^2$ being the position deviation relative to a reference path.

Taking the time derivative of z_i along (1), it follows that

$$\begin{aligned} \dot{z}_i =&d_i \begin{bmatrix} u_i \cos(\psi_i) - v_i \sin(\psi_i) \\ u_i \sin(\psi_i) + v_i \cos(\psi_i) \end{bmatrix} - \textstyle\sum_{j=1}^{N} a_{ij} R_j^T(\psi_j) \begin{bmatrix} u_j \\ v_j \end{bmatrix} \\ &- a_{i0} p_0^{\theta}(\theta)\dot{\theta} - d_i \dot{p}_{ijd}, \end{aligned} \tag{4}$$

where $d_i = \sum_{j=0}^{N} a_{ij}$; $R_j(\psi_j)$ is a rotation matrix given as $R_j(\psi_j) = \begin{bmatrix} \cos(\psi_j) & -\sin(\psi_j) \\ \sin(\psi_j) & \cos(\psi_j) \end{bmatrix}$.

Defining $\dot{\theta} = v_s - \varpi$ with v_s is a desired path update velocity; ϖ is a variable will be designed subsequently; (4) can be converted to a compact form as follows

$$\begin{aligned} \dot{z}_i =&d_i[u_i \cos(\psi_i), u_i \sin(\psi_i)]^T - a_{i0} p_0^{\theta}(\theta)(v_s - \varpi) \\ &+ \sigma_i, \end{aligned} \tag{5}$$

where $\sigma_i = -\sum_{j=1}^{N} a_{ij} R_j^T(\psi_j)[u_j, v_j]^T - d_i \dot{p}_{ijd} + d_i[-v_i \sin(\psi_i), v_i \cos(\psi_i)]^T$.

An ESO is used to estimate σ_i as follows

$$\begin{cases} \dot{\hat{z}}_i = d_i \begin{bmatrix} u_i \cos(\psi_i) \\ u_i \sin(\psi_i) \end{bmatrix} - a_{i0} p_0^{\theta}(\theta)(v_s - \varpi) + \hat{\sigma}_i \\ \qquad - K_{1i}^o(\hat{z}_i - z_i), \\ \dot{\hat{\sigma}}_i = -K_{2i}^o(\hat{z}_i - z_i), \end{cases} \tag{6}$$

where $K_{1i}^o \in \Re^2$ and $K_{2i}^o \in \Re^2$ are the observer gain matrices; $\hat{z}_i$, $\hat{\sigma}_i$ are the estimates of z_i, σ_i, respectively.

Assumption 2. There exists a positive constant σ_i^* such that $\|\dot{\sigma}_i\| \leq \sigma_i^*$.

Let $\tilde{z}_i = \hat{z}_i - z_i$ and $\tilde{\sigma}_i = \hat{\sigma}_i - \sigma_i$, (6) can be expressed as

$$\begin{cases} \dot{\tilde{z}}_i = \tilde{\sigma}_i - K_{1i}^o(\hat{z}_i - z_i), \\ \dot{\tilde{\sigma}}_i = -K_{2i}^o(\hat{z}_i - z_i) - \dot{\sigma}_i, \end{cases} \tag{7}$$

Defining $E_{i1} = [\tilde{z}_i^T, \tilde{\sigma}_i^T]^T \in \Re^4$, the equation (7) can be put into a matrix form as

$$\dot{E}_{i1} = A_i E_{i1} - B_i \dot{\sigma}_i, \tag{8}$$

where $A_i = \begin{bmatrix} -K_{1i}^o & 1 \\ -K_{2i}^o & 0 \end{bmatrix}, B_i = \begin{bmatrix} 0_2 \\ I_2 \end{bmatrix}$.

Because A_i is a Hurwitz matrix, there has a positive definite matrix P_{i1} satisfies the following equation:

$$A_i^T P_{i1} + P_{i1} A_i = -\varepsilon_i I_4, \tag{9}$$

where ε_i is a positive constant.

A distributed kinematic guidance law is designed as follows

$$\alpha_i = \Big(- \frac{K_i z_i}{\sqrt{\|z_i\|^2 + \Delta_i^2}} + a_{i0} v_s p_0^\theta(\theta) - \hat{\sigma}_i \Big) / d_i, \tag{10}$$

where $\alpha_i = [\alpha_{ix}, \alpha_{iy}]^T \in \Re^2$; $K_i = \mathrm{diag}\{k_{i1}, k_{i2}\} \in \Re^2$ is a kinematic gain matrix, $k_{i1} \in \Re$ and $k_{i2} \in \Re$ are positive constants; $\Delta_i \in \Re$ is a positive constants for avoiding large virtual control signal during transient; ϖ is updated as follows

$$\dot{\varpi} = -\lambda(\varpi + \mu \textstyle\sum_{i=1}^N a_{i0} (p_0^\theta(\theta))^T z_i), \tag{11}$$

where $\lambda \in \Re$ and $\mu \in \Re$ are positive constants.

The guidance signals are prescribed as

$$\begin{cases} \psi_{id} = \mathrm{atan2}(\alpha_{ix}, \alpha_{iy}) + 2k\pi, \\ u_{id} = \|\alpha_i\| \cos(\psi_{id} - \psi_i), \end{cases} \tag{12}$$

where k is a positive integral, $\mathrm{atan2}(\alpha_{ix}, \alpha_{iy})$ is the four-quadrant version of $\arctan(\alpha_{ix}/\alpha_{iy}) \in (-\pi/2, \pi/2)$.

As a consequence, the error subsystems can be expressed as follows

$$\begin{cases} \dot{z}_i = -\frac{K_i z_i}{\sqrt{\|z_i\|^2 + \Delta_i^2}} + a_{i0} p_0^\theta \varpi + e_i - \tilde{\sigma}_i, \\ \dot{\varpi} = -\lambda(\varpi + \mu \sum_{i=1}^N a_{i0} (p_0^\theta(\theta))^T z_i), \end{cases} \tag{13}$$

where $e_i = u_i(\cos\psi_i, \sin\psi_i)^T - u_{id}(\cos\psi_{id}, \sin\psi_{id})^T$. To move on, the following assumption is needed.

Assumption 3. The tracking error e_i is bounded by $\|e_i\| \leq l^*$ with l^* is a positive constant.

B. Stability analysis

The closed-loop system of kinematic guidance law can be regarded as a cascade system formed by the observer error dynamics (8) and the distributed formation error (13). The following lemmas state the input-to-state stability (ISS) of the subsystems (8) and (13).

Lemma 1. If Assumption 1 and 2 are satisfied, the system (8) viewed as a system with the state vector being E_{i1} and the input vector being $\dot{\sigma}_i$ is ISS.

Proof. Consider a Lyapunov function

$$V_{io} = \frac{1}{2} E_{i1}^T P_{i1} E_{i1}, \tag{14}$$

Taking the time derivative of V_{io} along (8), it follows that:

$$\dot{V}_{io} \leq -\frac{\varepsilon_i}{2} \|E_{i1}\|^2 + \|E_{i1}\| \|P_{i1} B_i\| \|\dot{\sigma}_i\|,$$

When E_{i1} satisfies

$$\|E_{i1}\| \geq \frac{2\|P_{i1} B_i\| \|\dot{\sigma}_i\|}{\varepsilon_i \bar{\theta}_{i1}}, \tag{15}$$

it renders $\dot{V}_{io} \leq -\frac{\varepsilon_i}{2}(1 - \bar{\theta}_{i1}) \|E_{i1}\|^2$, where $0 < \bar{\theta}_{i1} < 1$, it can be concluded that the subsystem (8) is ISS. Then there exists a class $\mathcal{KL}$ function γ_{i1} and a class $\mathcal{K}_\infty$ function κ_{i1} as follow, $\|E_{i1}(t)\| \leq \gamma_{i1}(\|E_{i1}(0)\|, t) + \kappa_{i1}(\|\dot{\sigma}_i\|)$.

Lemma 2. If Assumption 3 is satisfied, the subsystem (13), viewed as a system with the states being z_i, ϖ and the input being e_i, $\tilde{\sigma}_i$ is ISS.

Proof. Construct a Lyapunov function as

$$V_1 = \frac{1}{2} \textstyle\sum_{i=1}^N z_i^T z_i + \frac{\varpi^2}{2\lambda\mu}, \tag{16}$$

By differentiating V_1 along (13), it follows that

$$\dot{V}_1 = \textstyle\sum_{i=1}^N (-z_i^T K_i' z_i + z_i^T e_i - z_i^T \tilde{\sigma}_i) - \frac{\varpi^2}{\mu}, \tag{17}$$

where $K_i' = K_i / \sqrt{\|z_i\|^2 + \Delta_i^2}$.

Then, (17) can be rewritten as

$$\dot{V}_1 \leq -c\|E_1\|^2 + \|E_1\| \{ \textstyle\sum_{i=1}^N (\|e_i\| + \|\tilde{\sigma}_i\|) \}, \tag{18}$$

where $E_1 = [z^T, \varpi]^T$ with $z = [z_1^T, ..., z_N^T]$ and $c = \min_{i=1,...N}\{\lambda_{\min}(K_i'), \frac{1}{\mu}\}$.

As $\|E_1\| \geq \sum_{i=1}^N (\|e_i\| + \|\tilde{\sigma}_i\|)/c\bar{\theta}_1$, it renders $\dot{V}_1 \leq -c(1 - \bar{\theta}_1)\|E_1\|^2$, where $0 < \bar{\theta}_1 < 1$, it can be concluded that the subsystem (13) is ISS, and the ultimate bound is given by

$$\begin{aligned} \|E_1(t)\| \leq \max\{ & \|E_1(t_0)\| e^{-c(1-\bar{\theta}_1)(t-t_0)}, \\ & (\textstyle\sum_{i=1}^N (\|e_i\| + \|\tilde{\sigma}_i\|)/c\bar{\theta}_1)\}. \end{aligned} \tag{19}$$

Theorem 1. Under Assumptions 1-3, consider the ESO (6), the guidance law (10), and the path update law (11), the closed-loop system cascaded by the subsystem (8) and (13) is ISS.

Proof. Lemmas 1 and 2 have shown that the subsystem (8) with states E_{i1} and input vector being $\dot{\sigma}_i$ is ISS, and the subsystem (13) with states z_i, ϖ and input vector being e_i and $\tilde{\sigma}_i$ is ISS. As a result, the cascade system with states $\tilde{z}_i$, z_i, ϖ and exogenous input $\dot{\sigma}_i$, e_i, $\tilde{\sigma}_i$ is ISS. There exist a class $\mathcal{KL}$ function γ_1 and two class $\mathcal{K}_\infty$ function κ_1, κ_2 as follow, $\|E_2(t)\| \leq \gamma_1(\|E_2(0)\|, t) + \sum_{i=1}^N (\kappa_1\|\dot{\sigma}_i\| + \kappa_2\|e_i\|)$, where $E_2 = [\tilde{z}^T, z^T, \varpi]^T$. The proof is complete.

IV. Predictive Speed and Heading Control

This section presents the predictive speed and heading controller design.

A. Extended state observers

The heading and speed dynamics from (2) are

$$\begin{cases} \dot{u}_i = \zeta_{iu} + b_{iu}\tau_{iu}, \\ \dot{\psi}_i = r_i, \\ \dot{r}_i = \zeta_{ir} + b_{ir}\tau_{ir}, \end{cases} \tag{20}$$

where $b_{iu} = 1/m_{iu}$, $b_{ir} = 1/m_{ir}$; $\zeta_{iu} = [f_{iu}(u_i, v_i, r_i) + \tau_{iwu}(t)]/m_{iu}$; $\zeta_{ir} = [f_{ir}(u_i, v_i, r_i) + \tau_{iwr}(t)]/m_{ir}$.

Two ESOs are used for estimating the unknown states, system uncertainties and disturbances as follows

$$\begin{cases} \dot{\hat{u}}_i = \hat{\zeta}_{iu} + b_{iu}\tau_{iu} - 2\omega_{i1}(\hat{u}_i - u_i), \\ \dot{\hat{\zeta}}_{iu} = -\omega_{i1}^2(\hat{u}_i - u_i), \end{cases} \tag{21}$$

and

$$\begin{cases} \dot{\hat{\psi}}_i = \hat{r}_i - 3\omega_{i2}(\hat{\psi}_i - \psi_i), \\ \dot{\hat{r}}_i = \hat{\zeta}_{ir} + b_{ir}\tau_{ir} - 3\omega_{i2}^2(\hat{\psi}_i - \psi_i), \\ \dot{\hat{\zeta}}_{ir} = -\omega_{i2}^3(\hat{\psi}_i - \psi_i), \end{cases} \tag{22}$$

where $\omega_{i1} \in \Re$ and $\omega_{i2} \in \Re$ are parameters; $\hat{u}_i$, $\hat{r}_i$, $\hat{\psi}_i$, $\hat{\zeta}_{iu}$, and $\hat{\zeta}_{ir}$ are estimates of u_i, r_i, ψ_i, ζ_{iu}, and ζ_{ir}, respectively.

B. Finite-set model predictive speed controller

By using Euler discretization and the estimated information in (21), a prediction model of speed dynamics is given as

$$\hat{u}_i(k+1) = \hat{u}_i(k) + T_{is}(\hat{\zeta}_{iu} + b_{iu}\tau_{iu}(k)), \tag{23}$$

where $\tau_{iu}(k)$, $\hat{u}_i(k)$ denote the surge force and estimates of surge speed at k-th step; T_{is} is sampling time.

In order to track the speed reference u_{id} given by the kinematic guidance law, a cost function is given

$$\begin{aligned} J_{iu} = &\textstyle\sum_{i=1}^{N_p} \rho_{iu} \|\hat{u}_i(k+l|k) - u_{id}(k+l)\|^2 \\ &+ \textstyle\sum_{i=0}^{N_c-1} \beta_{iu} \|\tau_{iu}(k+l)\|^2, \end{aligned} \tag{24}$$

where N_p and N_c are the prediction horizon and the control horizon, respectively; $\hat{u}_i(k+l|k)$ is the l-th predicted output speed at k-th step; $u_{id}(k+l)$, $\tau_{iu}(k+l)$ denote the defined speed and control input at k-th step; $\rho_{iu} \in \Re$ and $\beta_{iu} \in \Re$ are control parameters.

The optimal control input τ_{iu} can be selected if the optimization problem can be solved:

$$\begin{cases} \tau_{iu}^{(k)} = \text{argmin} J_{iu}(\hat{u}_i, u_{id}, \tau_{iu}), \\ s.t. \hat{u}_i(k+1) = \hat{u}_i(k) + T_{is}(\hat{\zeta}_{iu} + b_{iu}\tau_{iu}(k)), \end{cases} \tag{25}$$

where $\tau_{iu}^{(k)} = \{\hat{\tau}_{iu}(k), \ldots \hat{\tau}_{iu}(k+N_c-1)\}$ is the optimal finite sets of τ_{iu} at k-th step. Only the first action $\hat{\tau}_{iu}(k)$ is applied.

C. Finite-set model predictive heading controller

By using Euler concretization and the estimated information in (22), a prediction model of heading dynamics is given as

$$\begin{cases} \hat{\psi}_i(k+1) = \hat{\psi}_i(k) + T_{is}\hat{r}_i(k+1), \\ \hat{r}_i(k+1) = \hat{r}_i(k) + T_{is}(\hat{\zeta}_{ir} + b_{ir}\tau_{ir}(k)), \end{cases} \tag{26}$$

where $\tau_{ir}(k)$, $\hat{\psi}_i(k)$ and $\hat{r}_i(k)$ denote the yaw moment, estimates of heading and angular rates at k-th step.

A cost function is designed as follows

$$\begin{aligned} J_{i\psi} = &\textstyle\sum_{i=1}^{N_p} \rho_{i\psi} \|\hat{\psi}_i(k+l|k) - \psi_{id}(k+l)\|^2 \\ &+ \textstyle\sum_{i=0}^{N_c-1} \beta_{i\psi} \|\tau_{ir}(k+l)\|^2, \end{aligned} \tag{27}$$

where $\hat{\psi}_i(k+l|k)$ is the l-th predicted output heading at k-th step; $\psi_{id}(k+l)$, $\tau_{ir}(k+l)$ denote the defined heading and control torque; $\rho_{i\psi} \in \Re$ and $\beta_{i\psi} \in \Re$ are optimization weights.

As a result, the optimal control torque can be obtained as

$$\begin{cases} \tau_{ir}^{(k)} = \text{argmin} J_{ir}(\hat{\psi}_i, \psi_{id}, \tau_{ir}), \\ s.t. \hat{\psi}_i(k+1) = \hat{\psi}_i(k) + T_{is}\hat{r}_i(k+1), \\ \hat{r}_i(k+1) = \hat{r}_i(k) + T_{is}(\hat{\zeta}_{ir} + b_{ir}\tau_{ir}(k)), \end{cases} \tag{28}$$

where $\tau_{ir}^{(k)} = \{\hat{\tau}_{ir}(k), \ldots \hat{\tau}_{ir}(k+N_c-1)\}$ is the optimal finite sets of τ_{ir} at k-th step, only the first part $\hat{\tau}_{ir}(k)$ is executed.

V. Simulation Results

Consider a network system consisting of five ASVs and one virtual leader. The communication graph of the network system can be found in Fig.2. The virtual leader is set to move along a parameterized path $p_0(\theta) = [0.06\theta + 3, 0.06\theta + 3]^T$. The formation pattern is set to $p_{1d} = [0, 0]^T$, $p_{2d} = [-5, 5]^T$, $p_{3d} = [5, -5]^T$, $p_{4d} = [-5, 5]^T$, $p_{5d} = [5, -5]^T$. The parameters for the proposed guidance law are set to $K_i = \text{diag}\{0.35, 0.35\}$, $\lambda = 10$, $\mu = 10$, $\Delta_i = 1$, $K_{1i}^o = \text{diag}\{60, 60\}$ and $K_{2i}^o = \text{diag}\{900, 900\}$. The parameters of the model predictive speed and heading controllers are set to $\omega_{i1} = 5$, $\omega_{i2} = 10$, $\rho_{iu} = 1$, $\beta_{iu} = 0$, $\rho_{i\psi} = 1$, $\beta_{i\psi} = 0$ and $T_{is} = 0.07$, the set of all τ_{iu}= $\{0, 0.5, 1, 1.5, 2, 2.5, 3, 3.5, 4, 4.5, 5, 5.5, 6, 6.5, 7, 7.5, 8, 8.5, 9, 9.5, 10\}$, and the set of torque τ_{ir} are selected as $\{-5, -4.5, -4, -3.5, -3, -2.5, -2, -1.5, -1, -0.5, 0, 0.5, 1, 1.5, 2, 2.5, 3, 3.5, 4, 4.5, 5\}$.

Simulation results are as shown in Fig.3-6. Fig.3 depicts the unmeasured speeds of neighboring ASVs can be estimated accurately. The errors of five ASVs in x-axis and y-axis are given in Fig.4. It can be seen the errors converge to a neighborhood of the zero. Fig.5 depicts the tracking performance of the predictive surge and heading controllers. Finally, Fig.6 shows the control input of ASV1.

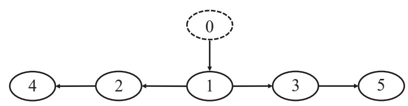

Fig. 2. Communication graph.

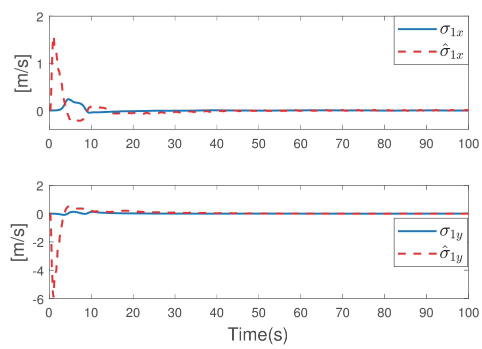

Fig. 3. The speed correlation estimation of neighbor about ASV1.

VI. CONCLUSIONS

This paper addressed the integrated distributed guidance and control for multiple under-actuated ASVs guided by a parameterized path. Each ASV subjects to unmeasured velocities of neighbors, system uncertainties and ocean disturbances. A robust distributed guidance and predictive control architecture is proposed. In the guidance loop, a robust distributed constant bearing guidance law is developed based on ESOs. In the control loop, predictive surge speed and heading controllers are designed where optimal actions are selected based on finite control sets and extended state observers. Simulation results demonstrate the effectiveness of the proposed robust distributed guidance and predictive control methods.

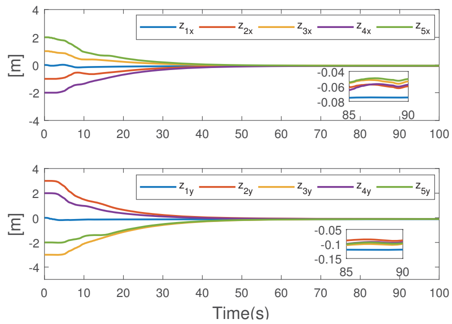

Fig. 4. Tracking errors of five ASVs in x-axis and y-axis.

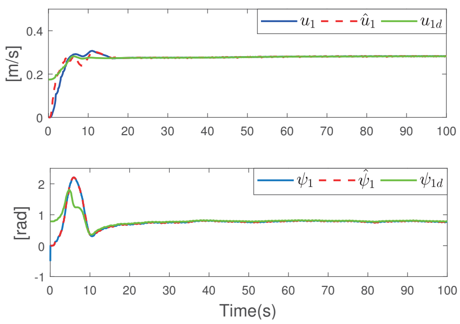

Fig. 5. Tracking performance of ASV1 using the linear heading ESO.

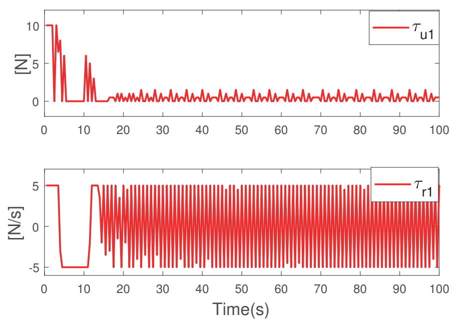

Fig. 6. Control inputs of ASV1 in the speed and yaw directions.

REFERENCES

[1] Z. Peng, J. Wang, and D. Wang, "Distributed containment maneuvering of multiple marine vessels via neurodynamics-based output feedback," *IEEE Transactions on Industrial Electronics*, vol. 65, no. 4, pp. 3831–3839, May 2017.

[2] ——, "Distributed maneuvering of autonomous surface vehicles based on neurodynamic optimization and fuzzy approximation," *IEEE Transactions on Control Systems Technology*, vol. 26, no. 3, pp. 1083–1090, May 2018.

[3] Z. Peng, D. Wang, T. Li, and M. Han, "Output-feedback cooperative formation maneuvering of autonomous surface vehicles with connectivity preservation and collision avoidance," *IEEE Transactions on Cybernetics*, 2019, DOI: 10.1109/TCYB.2019.2914717.

[4] Z. Peng, H. Wang, D. Wang, G. Sun, and H. Zhang, "Distributed model reference adaptive control for cooperative tracking of uncertain dynamical multi-agent systems," *IET Control Theory & Applications*, vol. 7, no. 8, pp. 1079–1087, May 2013.

[5] Z. Peng, D. Wang, and J. Wang, "Cooperative dynamic positioning of multiple marine offshore vessels: A modular design," *IEEE/ASME Transactions on Mechatronics*, vol. 21, no. 3, pp. 1210–1221, Jun. 2016.

[6] Z. Peng, D. Wang, Y. Shi, H. Wang, and W. Wang, "Containment control of networked autonomous underwater vehicles with model uncertainty and ocean disturbances guided by multiple leaders," *Information Sciences*, vol. 316, no. 12, pp. 163–179, Sep. 2015.

[7] Z. Peng, J. Wang, and D. Wang, "Containment maneuvering of marine surface vehicles with multiple parameterized paths via spatial-temporal decoupling," *IEEE/ASME Transactions on Mechatronics*, vol. 22, no. 2, pp. 1026–1036, Apr. 2017.

[8] Z. Peng, N. Gu, Y. Zhang, Y. Liu, D. Wang, and L. Liu, "Path-guided time-varying formation control with collision avoidance and connectivity preservation of under-actuated autonomous surface vehicles subject to unknown input gains," *Ocean Eningeering*, vol. 191, p. 106501, Nov 2019.

[9] N. Gu, D. Wang, Z. Peng, and L. Liu, "Distributed containment maneuvering of uncertain under-actuated unmanned surface vehicles guided by multiple virtual leaders with a formation," *Ocean Engineering*, vol. 187, no. 105996, 2019, DOI:10.1016/j.oceaneng.2019.04.077.

[10] Z. Peng and J. Wang, "Output-feedback path-following control of autonomous underwater vehicles based on an extended state observer and projection neural networks," *IEEE Transactions on Systems, Man, and Cybernetics: Systems*, vol. 48, no. 4, pp. 535–544, Apr. 2018.

[11] Z. Peng, J. Wang, D. Wang, and Q. long Han, "An overview of recent advances in coordinated control of multiple autonomous surface vehicles," *IEEE Transactions on Industrial Informatics*, 2020.

[12] F. Zhang, "Cyber-maritime cycle: Autonomy of marine robots for ocean sensing," *Foundations and Trends in Robotics*, vol. 5, no. 1, pp. 1–115, 2016.

[13] W. Wu, N. Gu, Z. Peng, D. Wang, and L. Liu, "Distributed time-varying formation control of marine surface vehicles guided by multiple leaders," *Chinese Journal of Ship Research*, pp. 1–10, 2020.

[14] X. Y. Z. Liu, Y. Zhang and C. Yuan, "Unmanned surface vehicles: An overview of developments and challenges," *Annual Reviews in Control*, vol. 41, pp. 71–93, 2016.

[15] M. Breivik, V. E. Hovstein, and T. I. Fossen, "Straight-line target tracking for unmanned surface vehicles," *Modeling, Identification and Control: A Norwegian Research Bulletin*, vol. 29, no. 4, pp. 131–149, 2008.

[16] L. Liu, D. Wang, Z. Peng, C. L. P. Chen, and T. Li, "Bounded neural network control for target tracking of underactuated autonomous surface vehicles in the presence of uncertain target dynamics," *IEEE Transactions on Neural Networks and Learning Systems*, vol. 30, no. 4, pp. 1241–1249, Apr. 2018.